Frontiers in Heat and Mass Transfer (FHMT), 20, 1 (2023)
DOI: 10.5098/hmt.20.1

Global Digital Central
ISSN: 2151-8629

Frontiers in Heat and Mass Transfer

Available at www.ThermalFluidsCentral.org

EFFECTS OF GEOMETRICAL AND FLOW PARAMETERS ON THE PERFORMANCE OF CROSS FLOW JET PLATE SOLAR AIR HEATER

Rajen Kumar Nayak[a,*], Ravi Shankar Prasad[a,†], Ujjwal Kumar Nayak[a], Amit Kumar Gupta[b]

[a] *Department of Mechanical Engineering, B.I.T. Sindri, Dhanbad, Jharkhand, PIN 828123, India*
[b] *Department of Chemical Engineering, B.I.T. Sindri, Dhanbad, Jharkhand, PIN 828123, India*

ABSTRACT

Inserting the jet plate between the bottom plate and absorber plate in a flat plate solar air heater has been proposed as an excellent option to enhance the performance of the conventional solar air heater. This research work presents an experimental study of flow and heat transfer in a jet plate solar air heater. Results are presented for the different mass flow rates of air $\dot{m}_1$ and $\dot{m}_2$, Reynolds number Re_{ja2}, streamwise pitch of the holes to jet hole diameter X/D, depth of upper channel to jet hole diameter Z_2/D, fixed number of jet hole N and angle of tilt θ. In the present study, it is found that outlet air temperature, collector efficiency, heat transfer coefficient and Nusselt number are higher at lower jet hole diameter, D (6 mm) as compared to higher jet hole diameter, D (8 mm and 10 mm) irrespective of the mass flow rates, $\dot{m}_1$ and $\dot{m}_2$. The outlet air temperature decreases with increase of mass flow rates of air ($\dot{m}_1$ and $\dot{m}_2$) and jet hole diameter. Based on the experimental data, the correlation for Nusselt number has been developed.

Keywords: air heater, cross flow, jet hole diameter, jet plate, solar, staggered hole

1. INTRODUCTION

In the solar energy applications, use of the conventional flat plate solar air heater is very common for drying of agricultural crops and space heating. In this system, the incoming solar radiation from the sun is incident on the absorber plate, which in turn transfers the heat to the flowing air by convection and surface radiation heat transfer (Sukhatme, 1996). In the last five decades, many new developments have been made in the solar air heating systems to improve its thermal performance as discussed in the following literatures.

Perry (1954) studied the convection heat transfer from a hot gas jet to a plane surface. Gupta and Garg (1967) presented the performance characteristics of four types of solar air heaters in an experimental study. Out of these four solar air heaters, two are corrugated type, while the other two are mesh type. Instead of the same rate of discharge, the same amount of pumping power was employed to take the unequal frictional losses into account for the comparison of the overall heater efficiency. The rating parameters like the plate efficiency factor, heat removal efficiency factor, overall heat loss coefficient and the effective absorption coefficient are also reported for the local weather conditions. Kercher and Tabakoff (1970) conducted an experimental investigation to study the heat transfer by multiple square arrays of round air jets impinging perpendicular to a flat surface including the effect of spent air. Correlations are developed for the Nusselt number in a semi-enclosed environment including the effects of the jet spent air flowing perpendicular to the jets as well as the effects of the jet diameter, jet spacing and jet to surface distance. Metzer et al. (1979) have found experimental results on heat transfer characteristics for inline and staggered arrays of circular jets with cross flow of spent air for various depth of the flow channel. The investigation shows that the Nusselt number is a strong function of Reynolds number. The result shows that the Nusselt number depends on the specific hole patterns as well as its spacings for the denser arrays. No significant enhancement in heat transfer coefficient is found with change in the depth of flow channel. Florschuetz et al. (1981) have observed the behaviour of heat transfer coefficient in inline and staggered hole jet plate for various pitch of the jet holes. The heat transfer coefficient in staggered hole jet plate is found higher than inline hole jet plate for fixed jet hole diameter. Garg et al. (1983) studied the effect of enhanced heat transfer area in solar air heaters. Prasad and Saini (1988) studied the effect of artificial roughness on heat transfer and friction factor in a solar air heater. Garg et al. (1989) studied the performance of a fin type solar air heater, both experimentally and theoretically. In the experimental setup, the fins are attached with the upper plate of the conventional duct type solar air heater with single glazing. The experiments are performed on two clear days for the two different mass flow rates. Garg et al. (1990) evaluated the performance of a duct type solar air heater with rectangular fins in the air flow passage between the absorber and the rear plate. The mathematical model developed predicted the effects of the different design and operational parameters on the thermal performance of the solar air heater. The shallower duct depth as well as the increased number and length of the rectangular fins improve the performance of the air heater, but increase the pressure drop also. Thus, the energy expended in pumping the air through the collector in increased.

Garg et al. (1991) made a numerical simulation of the theoretical model to evaluate the effect of the number of rectangular fins, the length of the fins, the depth of the air channel and the air flow rate on the thermal performance of the solar air heater. These results are compared with the results for a conventional solar air heater with the same duct depth and length. The outlet air temperature and total thermal energy collected are increased with an increase in the number of fins and decrease in the duct depth, while all other design and operational parameters are kept constant. The shallower duct depth improves the thermal performance of

[*] Department of Mechanical Engineering, B.I.T. Sindri, Dhanbad, Jharkhand, PIN 828123, India
[†] *Corresponding author. Email: rsprasad.me@bitsindri.ac.in*

Global Digital Central
ISSN: 2151-8629

the solar air heater, but increases the pressure drop also. Garg et al. (1990, 1991) accounted this expended energy by introducing a new term 'effective heat gain', which is computed and compared for the different cases separately. Chaudhury and Garg (1991) have done analytical study in cross flow and non-cross flow inline hole jet plate solar air heater for varying mass flow rates of air, jet hole diameter, depth of the channel and pitch of the jet holes. The gain in air temperature increment in non-cross flow jet plate over the parallel plate air heater is found as 9.5°C and 15.5°C for depth (Z), 0.05m and 0.10m respectively at fixed mass flow rate of air $\dot{m}_1$ (50.0 kg/hm^2). The effects of various geometrical parameters i.e., the hole or nozzle diameter on the jet plate, their interspacing, the nozzle's height, the distance between the absorber and the jet plate and the other operational parameters such as the velocity of the air impinging out of the holes or nozzles on to the back side of the absorber surface is investigated on the performance parameters of the jet impingement concept solar air heater. A detailed theoretical parametric analysis is made on the design for different mass flow rates of air and different lengths of air channel. Verma et al. (1991) presented a detailed theoretical parametric analysis of a corrugated solar air heater with and without cover. The flow channel depth is optimized for the maximum availability of heat at the lowest collector cost. The effect of collector parameters and operating conditions on the collector performance is analyzed. Gupta et al. (1993) studied heat and fluid flow in rectangular solar air heater ducts having transverse rib roughness on absorber plates. This experimental investigation was carried out for the solar air heater ducts with absorber plates having transverse wire roughness in transitionally rough flow region. Thombre and Sukhatme (1995) studied the turbulent flow heat transfer and friction factor characteristics of shrouded fin arrays with uninterrupted fins.

Sahu and Bhagoria (2005) made augmentation of heat transfer coefficient by using 90° broken transverse ribs on absorber plate of solar air heater. Irfan and Emre (2006) made an experimental investigation of solar air heater with free and fixed fins. Jaurker et al. (2006) studied heat transfer and friction characteristics of solar air heater duct using rib-grooved artificial roughness. Kurtbas and Turgut (2006) made an experimental investigation of solar air heater with free and fixed fins. Singh (2006) conducted the performance studies on continuous longitudinal fins solar air heater. Prasad and Saini (1988), Sahu and Bhagoria (2005) and Jaurker et al. (2006) have performed experimental work for checking the performance of the parallel plate solar air heater and also developed the correlations for Nusselt number and friction factor at different flow conditions in the flow channel having roughness of different shapes and sizes. Karsli (2007) made a performance analysis of new design of solar air collectors for drying applications. Romdhane (2007) made a comparative study of the air solar collectors and studied the heat transfer with the introduction of baffles to favor the heat transfer. Belusko et al. (2008) have experimentally investigated the performance of the jet impingement unglazed solar air heater for different width of collector and pitch of the jet holes. The increment in thermal efficiency is found as 21.0% in jet impingement unglazed air collector in comparison to the parallel plate solar air heater. Aharwal et al. (2009) presented the effect of artificial roughness of the absorber surface on the heat transfer and friction factor in a parallel plate solar air heater. The maximum enhancement in Nusselt number and friction factor as a result of providing artificial roughness have been found as 2.30 and 2.83 times respectively as compared to the smooth duct for an angle of attack of 60°. The correlations for Nusselt number and friction factor are developed as a function of roughness parameters of inclined discrete square ribs and flow Reynolds number. Akpinar and Kocyigit (2010) made an experimental investigation of thermal performance of solar air heater having different obstacles on absorber plates. Xing et al. (2010) made an experimental and numerical investigation of heat transfer characteristics of inline and staggered arrays of impinging jets.

Chabane et al. (2013a) analyzed the collector efficiency by single pass of solar air heaters with and without using fins. Chabane et al. (2013b) performed a thermal efficiency analysis of a single flow solar air heater with different mass flow rates in a smooth plate. Chauhan and Thakur (2013) developed correlations for Nusselt number and friction factor in cross flow inline hole jet solar air heater for different jet hole diameter and pitch of the jet holes. The developed correlations show the Nusselt number is a strong function of Reynolds number. Chabane et al. (2014) made an experimental study of heat transfer and thermal performance with longitudinal fins of solar air heater. Nayak and Singh (2016) carried out an experimental investigation showing the effects of channel spacing between jet plate and absorber plate on the performance of cross flow staggered hole jet plate solar air heater. Aboghrara et al. (2017) made a performance analysis of solar air heater with jet impingement on corrugated absorber plate. Hasan et al. (2017) performed an experimental investigation of jet array nanofluids impingement in photovoltaic and thermal collector. In this experimental study, the effect of nanoparticles (SiC, TiO_2 and SiO_2) with water as its base fluid on the electrical and thermal performance of a photovoltaic thermal collector equipped with jet impingement was studied. Nadda et al. (2017) studied heat transfer and friction loss in an impingement jets solar air heater with multiple arc protrusion obstacles. Rajaseenivasan et al. (2017) made an experimental investigation on the performance of an impinging jet solar air heater. Soni and Singh (2017) made an experimental analysis of geometrical parameters on the performance of an inline jet plate solar air heater. Vinod and Singh (2017) analyzed the thermo-hydraulic performance of jet plate solar air heater under cross flow condition. Aboghrara et al. (2018) made a parametric study on the thermal performance and optimal design elements of solar air heater enhanced with jet impingement on a corrugated absorber plate. Matheswaran et al. (2018) presented an analytical investigation of solar air heater with jet impingement using energy and exergy analysis. Sivakumar et al. (2019) made an experimental thermodynamic analysis of a forced convection solar air heater using absorber plate with pin fins. Kumar et al. (2020) developed the new correlations for heat transfer and pressure loss due to internal conical ring obstacles in an impinging jet solar air heater passage. Singh et al. (2020) utilized circular jet impingement to enhance thermal performance of solar air heater. Yadav and Saini (2020) made a numerical investigation on the performance of a solar air heater using jet impingement with absorber plate.

Farahani and Shadi (2021) made an economic, energetic and exergetic optimization of roughened solar collectors with and without impingement jet. It is observed that the existence of jet plate increases the heating power and temperature difference significantly. Hassan and AboElfadl (2021) made a heat transfer and performance analysis of solar air heater having new transverse finned absorber of lateral gaps and central holes. Kumar et al. (2021a) developed the heat transfer and friction factor correlations for an impinging air jets solar thermal collector with arc ribs on an absorber plate. Kumar et al. (2021b) made a comprehensive review of performance analysis of solar thermal collector with and without fins. The improvement in the thermal performance by attaching the fins of various design, shapes and geometry underside the absorber plate of the single pass and double pass solar thermal collector is discussed. The influence of various fins on turbulence, heat transfer and other performance parameters is discussed. The comparative study in literature review suggests that the heat transfer rate for the solar air thermal collector with fins is significantly greater in comparison with the solar air thermal collector without fins. Maithani et al. (2021) made a thermo-hydraulic and exergy analysis of inclined impinging jets on absorber plate of solar air heater. Moshery et al. (2021) analyzed the thermal performance of jet impingement solar air heater with transverse ribs absorber plate. Pazarlioğlu et al. (2021) made a numerical analysis of effect of impinging jet on cooling of solar air heater with longitudinal fins. Salman et al. (2021a) made an exergy analysis of solar heat collector with air jet impingement on dimple shaped roughened absorber surface. Salman et al. (2021b) performed an experimental analysis of single loop solar heat collector with jet impingement over indented dimples. Shetty et al. (2021) made a numerical analysis of a solar air heater with circular perforated absorber plate.

Global Digital Central
ISSN: 2151-8629

Das et al. (2022) made a numerical analysis of a solar air heater with jet impingement and the comparison of performance between jet designs. Flilihi et al. (2022) studied the effect of absorber design on convective heat transfer in a flat plate solar collector through the CFD modeling. Nayak et al. (2022a) presented an analytical study of thermal performance of a jet plate solar air heater with the longitudinal fins under the cross flow and non-cross flow conditions. Nayak et al. (2022b) presented a performance analysis of longitudinal fin jet plate solar air heater under cross flow condition. The empirical correlations for Nusselt number, friction factor and fin effectiveness have been developed based on the experimental data. Salman et al. (2022) utilized jet impingement on protrusion or dimple heated plate to improve the performance of double pass solar heat collector. The effect of different geometrical parameters of jet impingement on indented protrusion of protruded absorber plate in double-pass solar heat collector is investigated. Yadav and Saini (2022) made a thermo-hydraulic CFD analysis of impinging jet solar air heater with different jet geometries. This study analyzed the thermal behaviour of impinging jet solar air heater with five different jet geometries such as triangular, rectangular, square, hexagonal and circular jet. Heat transfer as Nusselt number and pumping loss as friction factor has been analyzed and compared for all the geometries under identical operating conditions.

Based on the above cited literatures, it is found that no detailed literatures are available on experimental work showing the influence of staggered jet hole diameter on the performance of jet plate solar air heater and also no empirical correlations are presented. Nayak and Singh (2016) presented the influence of gap between absorber plate and jet plate, Z_2 on the performance of the solar air heater. However, they have not investigated the effect of jet hole diameter in the above case. So, the present study focuses on the effect of jet hole diameter with fixed channel spacing between jet and absorber plate (Z_2) on the performance of the solar air heater. In this investigation, the correlations for Nusselt number as the functions of Re_{ja2}, X/D and Z_2/D have also been developed, which complies as one of the contributions of the present work.

2. DESCRIPTION OF EXPERIMENTAL SET UP AND PROCEDURE

The photographic, schematic and sectional view of the experimental set up are shown in Figs. 1(a), 1(b) and 1(c), whereas the pictorial view of the staggered hole jet plate placed between bottom plate and absorber plate is presented in Fig. 2. The experimental set up consists of blower, dull black painted absorber plate, bottom plate, jet plate with staggered hole, toughened glass cover plate, voltage regulator, three numbers of digital temperature display units (DTDU) and thermocouples embedded on each plate. The sides and bottom of the air heater are properly insulated with glass wool for reducing the side and bottom heat losses.

The specifications of the solar air heater are shown in Table 1. The total numbers of the circular holes (D = 6.0mm-10.0 mm) are 1173, which are fixed for all cases and arranged in a staggered manner in the jet plate. The total depth, Z between absorber and bottom plate is 14.0 cm which is divided into two separate flow channels by inserting the jet plate between the absorber and bottom plate of the solar air heater. The depth of bottom channel, Z_1 and upper channel, Z_2 are kept same and equal to 7.0 cm. Three drilled holes, one each in the inlet side of the lower and upper channel and one exit side are made for inserting the probe of the Digital Hot Wire Anemometer (DHWA). The whole structure is supported on a movable steel frame at a fixed tilt angle.

The mass flow rate in the inlet air at bottom channel, $\dot{m}_1$ and upper channel, $\dot{m}_2$ of the solar air heater is supplied by a single axial blower regulated by a voltage regulator. The mass flow rate of air $\dot{m}_1$ impinging out from the holes in jet plate is mixed with $\dot{m}_2$ and exits from the upper channel. The inlet velocity $\overline{VV}_1$ and $\overline{V}_2$ in the lower and upper channels respectively, outlet velocity $\overline{V}$ and velocity of the mixed air in the upper channel $\overline{V}$ $\overline{V}_o$ is measured by DHWA. The same instrument is used for measuring the inlet air temperature, T_i and outlet air temperature, T_o of the mixed air. The accuracy of the instrument, DHWA is ±0.05 m/s (velocity) and ±0.8ºC (temperature) with the range of operating temperature 0ºC to 50ºC. The temperatures of absorber plate (T_P), jet plate (T_j) and bottom plate (T_b) are measured by the thermocouples having accuracy ±2.2ºC or 0.4 % with the range of operating temperature is 0ºC to 1250ºC. The total ten numbers of thermocouple are embedded on the lower and upper surface of the absorber plate and jet plate. However, total three numbers of thermocouple are embedded on the bottom plate. During all the experiments, the solar intensity (I_T) has been recorded by using a pyranometer coupled with a digital millivoltmeter of accuracy less than ±1.0%. The tilt angle, θ of the solar air heater is given 22.6º with respect to the horizontal surface.

This experimental works has been carried out in the winter season during 09:00 A.M. - 03:00 P.M. in the clear sky at IIT (ISM) Dhanbad, Jharkhand, India.

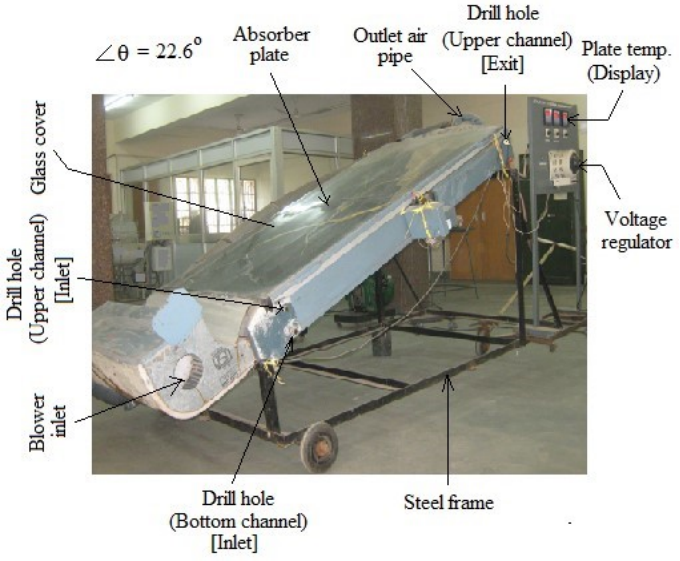

Fig. 1(a) Photographic view of the experimental setup

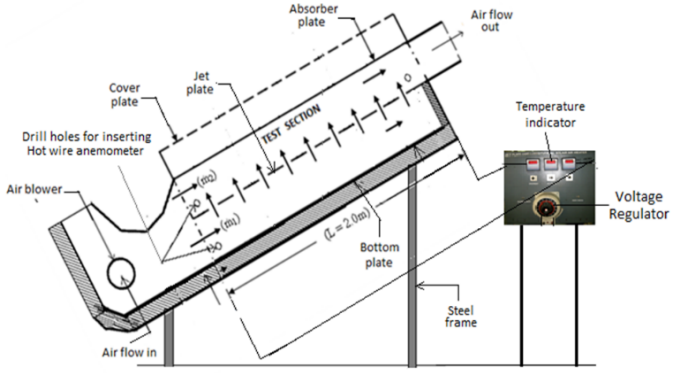

Fig. 1(b) Schematic view of the experimental setup

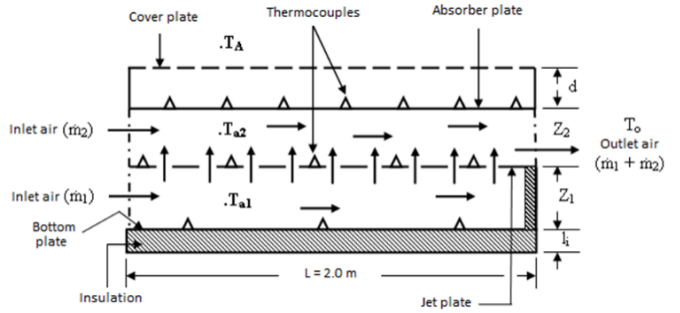

Fig. 1(c) Sectional view of air heater showing air flow in channels for cross flow condition

Global Digital Central
ISSN: 2151-8629

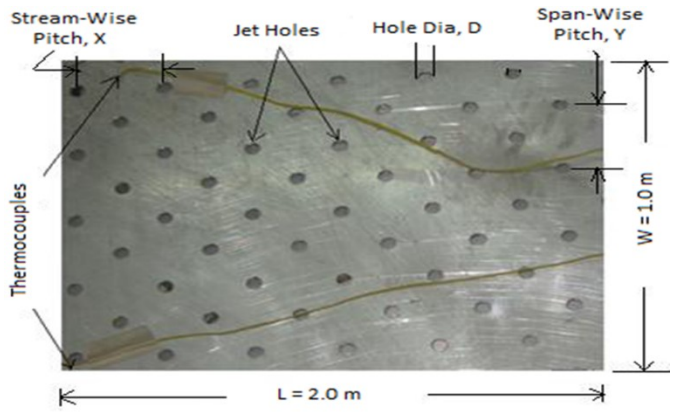

Fig. 2 Photographic view of the jet plate with staggered hole

Table 1 Specifications of the solar air heater

Dimension	*Specifications*
Length of solar air heater, L	L = 2.0 m
Width of collector, W	W = 1.0 m
Streamwise pitch of the holes, X	X = 43 mm
Spacing between bottom and jet plate, Z_1	Z_1 = 7 cm
Spacing between jet and absorber plate, Z_2	Z_2 = 7 cm
Jet hole diameter in jet plates, D	D = 6 mm, 8 mm, 10mm
Absorber plate thickness, t	t = 1.0 mm
Absorptivity	α = 0.95
Jet plate thickness, t (Material: Al-alloy)	t = 4.0 mm
Glass cover thickness, t and transmissivity, τ (Material: Toughened glass)	t = 4 mm, τ = 0.95
Thickness of insulation (Material: Glass wool)	l_i = 2.5 cm
Air thickness, d	d = 2.54 cm
Tilt angle, θ	θ = 22.6°

3. DATA REDUCTION

The experimental data for jet plate, absorber plate, bottom plate and air temperatures at various locations in the flow channel have been recorded under steady state conditions for given jet hole diameter (D), mass flow rates of air ($\dot{m}_1$ and $\dot{m}_2$) and solar intensity (I_T). The collected data have been used for computing the heat transfer coefficient (h_{Pj}), collector efficiency (η_c), flow Reynolds number (Re_{ja2}), Nusselt number (Nu_{Pj}) and friction factor (f_s) for the given set up. In order to calculate h_{Pj}, η_c, Re_{ja2}, Re_D, Nu_{Pj} and f_s, the following equations are used under steady state condition.

$$h_{Pj} = (\dot{m}_1 + \dot{m}_2)\, C_p\, (T_o - T_i) / A\, (T_P - T_{a2}) \quad (1)$$

where $T_i = (\dot{m}_1 T_1 + \dot{m}_2 T_2) / (\dot{m}_1 + \dot{m}_2)$

and $T_{a2} = [\dot{m}_1 T_1 + \dot{m}_2 T_2 + (\dot{m}_1 + \dot{m}_2)\, T_o] / 2(\dot{m}_1 + \dot{m}_2)$

Collector efficiency, $\eta_c = (\dot{m}_1 + \dot{m}_2)\, C_p\, (T_o - T_A) / I_T A \quad (2)$

Reynolds number in upper channel, $Re_{ja2} = \rho \overline{V} D_2 / \mu \quad (3)$

where $\overline{V} = (\overline{V}_{av} + \overline{V}_o) / 2$, $\overline{V}_{av} = (A_j V_j + A_2 \overline{V}_2) / (A_2 + A_j)$,

$A_2 = W Z_2$ and $V_j = 4\dot{m}_1 / N\rho\pi D^2$

Nusselt number in upper channel, $Nu_{Pj} = h_{Pj} D_2 / k_a \quad (4)$

4. UNCERTAINITY ANALYSIS

Kline and Klintock method (1953) has been used for finding the total uncertainties (precision and bias) in heat transfer coefficient (h_{Pj}), collector efficiency (η_c) and flow Reynolds number (Re_{ja2}), which are mainly related with ($\dot{m}_1$, $\dot{m}_2$, T_o, T_i, T_P, T_{a2}), ($\dot{m}_1$, $\dot{m}_2$, T_A, T_o, I_T) and (ρ, V_j, $\overline{V}_2$, $\overline{V}_o$) respectively. However, $\dot{m}_1$ is related with the density, ρ of air and $\overline{V}_1$. Similarly, $\dot{m}_2$ is related with density, ρ of air and $\overline{V}_2$ and density, ρ with temperature, T_A. Hence, the total uncertainties of h_{Pj}, η_c and Re_{ja2} are related with (T_A, $\overline{VV}_1$, $\overline{V}_2$, T_o, T_i, T_P, T_{a2}), (T_A, $\overline{VV}_1$, $\overline{V}_2$, T_o, I_T) and (T_A, V_j, $\overline{V}_2$, $\overline{V}_o$) respectively.

The total uncertainties in h_{Pj}, η_c, Re_{ja2}, T_A, T_i, T_o, $\overline{VV}_1$, $\overline{V}_2$, $\overline{V}_o$ and I_T are found as ±0.71%, ±0.04%, ±0.21%, ±0.64%, ±0.18%, ±0.08%, ±0.03%, ±0.02%, ±0.03% and ±0.23% respectively.

Uncertainty formulation (Moffat, 1988) is presented in Appendix A.

5. RESULTS AND DISCUSSION

5.1 Effect of mass flow rates of air ($\dot{m}_1$ and $\dot{m}_2$) and jet hole diameter (D) on outlet air temperature (T_o) and collector efficiency (η_c)

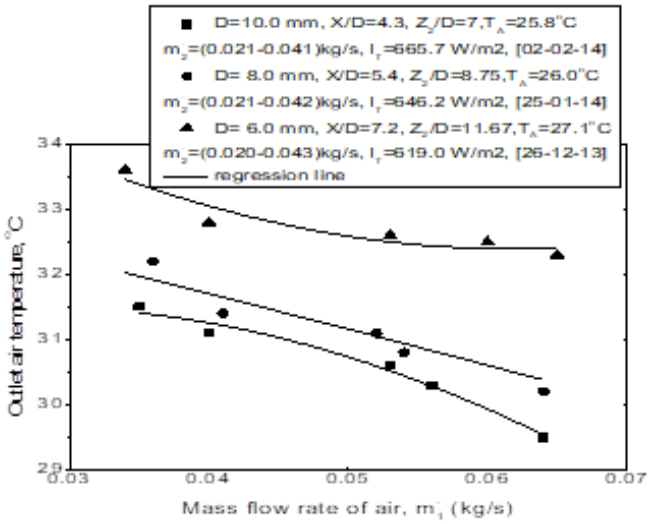

Fig. 3 Variation of outlet air temperature with mass flow rates of air (m_1 and m_2) and jet hole diameter (D) in cross flow staggered hole jet plate solar air heater for X/D (4.3-7.2) and Z_2/D (7.0-11.67)

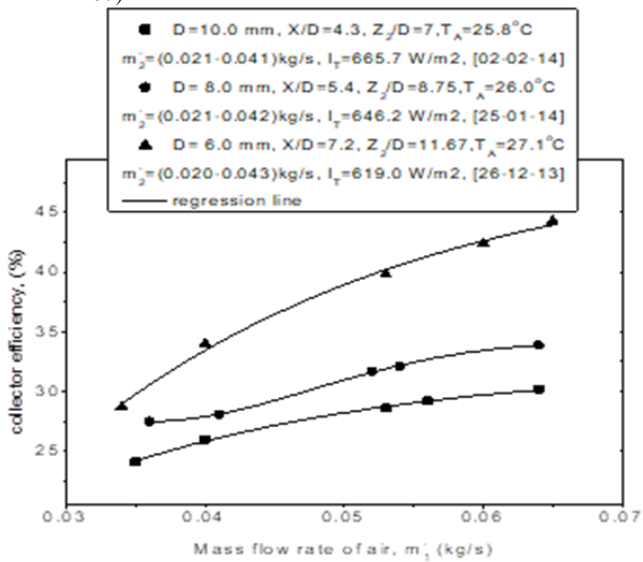

Fig. 4 Variation of collector efficiency with mass flow rates of air (m_1 and m_2) and jet hole diameter (D) in cross flow staggered hole jet plate solar air heater for X/D (4.3-7.2) and Z_2/D (7.0-11.67)

Global Digital Central
ISSN: 2151-8629

Figures 3 and 4 show the outlet air temperature (T_o) decreases and the collector efficiency (η_c) increases with increase in mass flow rates of air ($\dot{m}_1$ and $\dot{m}_2$) for fixed X/D and Z_2/D. It is observed that the outlet air temperature (T_o) and collector efficiency (η_c) are higher for small jet hole diameter D (6.0 mm), fixed streamwise pitch of the holes, X (43.0 mm), depth of channel Z_1 (7.0 cm) and Z_2 (7.0 cm) due to high jet air velocity (Vj). The air with the high jet velocity strikes the lower surface of the absorber plate and breaks the thermal boundary layer of the surface resulting in increment in heat transfer coefficient, h_{Pj} leading to enhancement in outlet air temperature and collector efficiency for all range of mass flow rates of air $\dot{m}_1$ and $\dot{m}_2$. The collector efficiency increases with increase in mass flow rate due to increment of heat transfer from the absorber plate (McAdams, 1954). For $\dot{m}_1$ (0.04 kg/s) and X/D (4.3-7.2), the increment of outlet air temperaure (T_o) and collector efficiency (η_c) are obtained as 4.46% and 21.4% higher in smaller jet hole diameter, D (6.0 mm) as compared to larger jet hole diameter, D (8.0 mm). Further, the increment of outlet air temperature and collector efficiency are found as 5.47% and 30.8% higher in smaller jet hole diameter, D (6.0 mm) with respect to larger jet hole diameter, D (10.0 mm). Even at lower I_T (619.0 W/m^2), the maximum gain in the outlet air temperature is observed as 1.6°C and 2.2°C for smaller jet hole diameter, D (6.0 mm). Similarly, the maximum gain in collector efficiency is found as 10.5% and 14.9% respectively, for the smaller jet hole diameter, D (6.0 mm) at mass flow rate of air $\dot{m}_1$ (0.064 kg/s) and X/D (4.3-7.2).

5.2 Effect of mass flow rates of air ($\dot{m}_1$ and $\dot{m}_2$) and jet hole diameter (D) on heat transfer coefficient of absorber plate-to-jet air (h_{Pj})

Figure 5 shows that the effect of mass flow rates of air ($\dot{m}_1$ and $\dot{m}_2$) and jet hole diameter on heat transfer coefficient of absorber plate-to-jet air (h_{Pj}) in cross flow staggered hole jet plate solar air heater for fixed streamwise pitch, X (43.0 mm) and reveals that the heat transfer coefficient, h_{Pj} increases with decrease in jet hole diameter for mass flow rates of air ($\dot{m}_1$ and $\dot{m}_2$) and X/D (4.3-7.2). Even at lower I_T (619.0 W/m^2), the heat transfer coefficient, h_{Pj} is found higher at smaller jet hole diameter, D (6.0 mm) for fixed mass flow rates of air ($\dot{m}_1$ and $\dot{m}_2$) and X/D (4.3-7.2). The higher h_{Pj} in lower jet hole diameter is due to high jet air velocity (Vj) through the jet hole. This higher value of heat transfer coefficient of plate to jet air, h_{Pj} leads to increment in outlet air temperature and collector efficiency. For fixed mass flow rate, $\dot{m}_1$ (0.064 kg/s) and X/D (4.3-7.2), the maximum increment of h_{Pj} is found as 57.9% and 82.9% higher at lower jet hole diameter, D (6.0 mm) than higher jet hole diameters, D (8.0 mm) and D (10.0 mm) respectively.

5.3 Effect of mass flow rates of air ($\dot{m}_1$ and $\dot{m}_2$) and jet hole diameter (D) on Nusselt number (Nu_{Pj})

Figure 6 shows that the Nusselt number (Nu_{Pj}) increases with increase in mass flow rates of air $\dot{m}_1$ and $\dot{m}_2$, whereas the Nusselt number decreases with increase in jet hole diameter (D) for X/D (4.3-7.2) and Z_2/D (7.0-11.67). For fixed mass flow rates of air ($\dot{m}_1$ and $\dot{m}_2$) and X/D (4.3-7.2), the Nusselt number is found substantially higher at smaller jet hole diameter, D (6.0 mm) as compared to larger jet hole diameter, D (8.0 mm and 10.0 mm) due to formation of high jet air velocity, Vj through the jet holes. The high jet air velocity creates more turbulence in the air within the channel resulting in increment in heat transfer coefficient (h_{Pj}) and Nusselt number (Nu_{Pj}). The Nusselt number increases with increase in mass flow rates of air ($\dot{m}_1$ and $\dot{m}_2$) due to high air flow velocity ($\overline{V}$) in the channel, which leads to increment in heat transfer coefficient (h_{Pj}) and Nusselt number (Nu_{Pj}). For $\dot{m}_1$ (0.064 kg/s), X/D (4.3-7.2) and Z_2/D (7.0-11.67), the maximum increment of Nusselt number (Nu_{Pj}) are found as 52.6% and 75.0% for lower jet hole diameter, D (6.0 mm) with respect to higher jet hole diameter, D (8.0 mm) and D (10.0 mm).

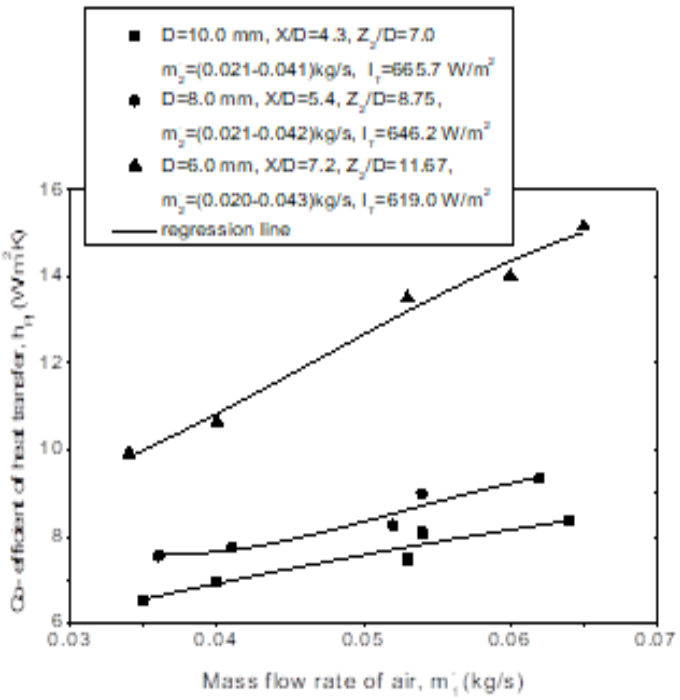

Fig. 5 Variation of coefficient of heat transfer (h_{Pj}) with mass flow rates of air (m_1 and m_2) and jet hole diameter (D) for X/D (4.3-7.2) and Z_2/D (7.0-11.67)

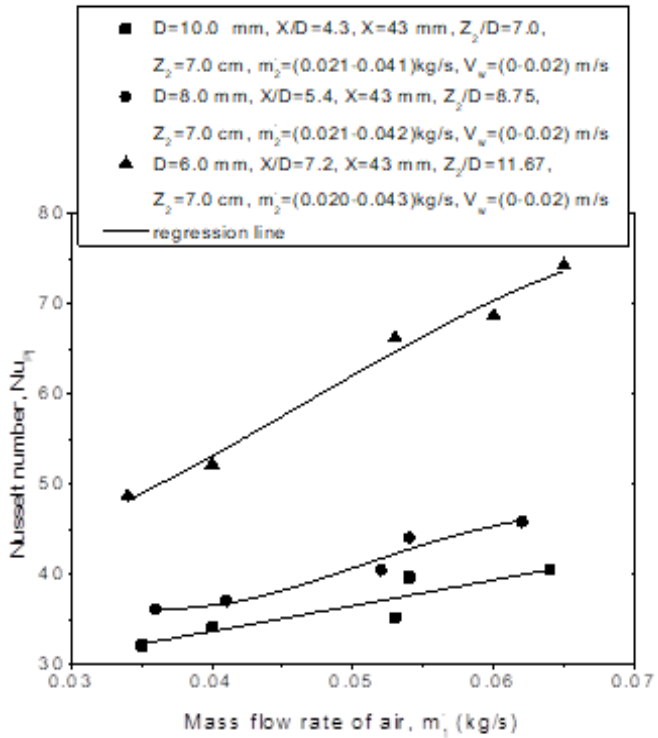

Fig. 6 Variation of Nusselt Number (Nu_{Pj}) with mass flow rates of air m_1 and m_2 for X/D (4.3-7.2) and Z_2/D (7.0-11.67)

Global Digital Central
ISSN: 2151-8629

5.4 Variation of Nusselt number (Nu_{Pj}) with Reynolds number (Re_{ja2})

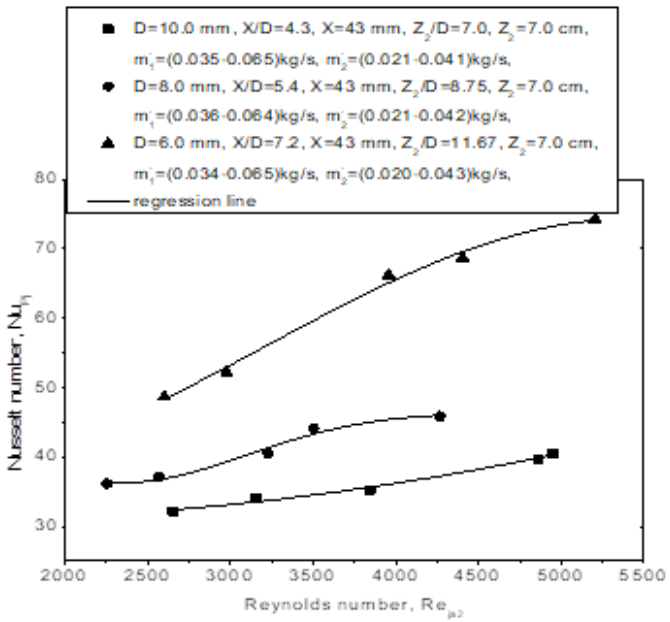

Fig. 7 Variation of Nusselt number (Nu_{Pj}) with Reynolds number (Re_{ja2}) in cross flow staggered hole jet plate solar air heater for X/D (4.3-7.2)

The variation of Nusselt number with Reynolds number (Re_{ja2}) is presented in Fig. 7. The Nusselt number (Nu_{Pj}) increases with increase in Reynolds number (Re_{ja2}) in jet plate solar air heater for fixed X/D and Z_2/D. For all range of Reynolds number (Re_{ja2}), X/D and Z_2/D, the Nusselt number has been found higher in lower jet hole diameter, D (6.0 mm), because of getting higher jet air velocity (V_j) for lower jet hole diameter resulting in increment of Nusselt number of jet plate solar air heater. The Nusselt number increases with the increase in Reynolds number due to increase of turbulence in the air, which results to increment of heat transfer from the absorber plate. The maximum increment in Nusselt number (Nu_{Pj}) are found as 18.52% and 26.33% at jet hole diameter, D (6.0 mm) with respect to jet hole diameter, D (8.0 mm) and D (10.0 mm) respectively for X/D (4.3-7.2) and Z_2/D (7.0-11.67), whereas the maximum increment of Nusselt number are obtained 45.8% and 83.7% in jet hole diameter, D (6.0 mm) than the jet hole diameter D (8.0 mm) and D (10.0 mm) respectively at Re_{ja2} (4265.0), X/D (4.3-7.2) and Z_2/D (7.0-11.67) in jet plate solar air heater.

5.5 Correlations

In the present work, the range of parameters for correlations are considered as $2600 \le Re_{ja2} \le 5200$, $4.3 \le X/D \le 7.2$, $7.0 \le Z_2/D \le 11.67$. Based on a large set of experimental data, the following new empirical correlations are presented.

5.5.1 Correlation for Nusselt number (Nu_{Pj})

$$Nu_{Pj} = 0.0248\ (Re_{ja2})^{0.7609}\ (X/D)^{0.6204}\ (Z_2/D)^{0.0634} \quad (5)$$

Reynolds number (Re_{ja2}) directly affects the Nusselt number (Nu_{Pj}) and its positive exponent shows that the Nusselt number (Nu_{Pj}) increases with increase of Reynolds number (Re_{ja2}) in the jet plate solar air heater. The positive exponent of the terms (X/D) and (Z_2/D) indicate the Nusselt number (Nu_{Pj}) increases with increase in streamwise pitch of the holes (X) and depth of channel (Z_2) for fixed jet hole diameter (D). It also signifies that the Nusselt number (Nu_{Pj}) increases with decrease in the jet hole diameter (D) for the fixed values of X and Z_2. The value of correlation coefficient 0.90 indicates the goodness of fit as shown in the Fig. 8.

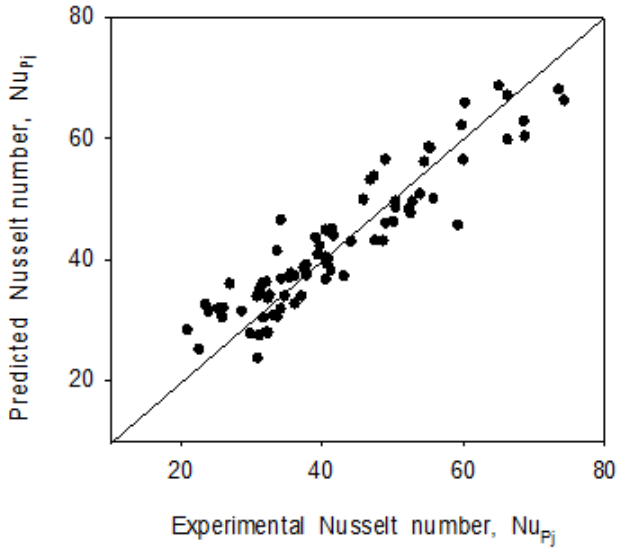

Fig. 8 Parity plot between predicted and experimental values of Nusselt number for X/D (4.3-7.2) and Z_2/D (7.0-11.67)

6. CONCLUSIONS

In the present paper, an experimental investigation has been reported analyzing the effect of mass flow rates of air ($\dot{m}_1$ and $\dot{m}_2$) and jet hole diameter (D) on the performance of jet plate solar air heater. For all range of mass flow rates of air ($\dot{m}_1$ and $\dot{m}_2$), X/D (4.3-7.2) and Z_2/D (7.0-11.67), it has been found that the outlet air temperature (T_o), collector efficiency (η_c), coefficient of heat transfer (h_{Pj}) and Nusselt number (Nu_{Pj}) are higher for smaller jet hole diameter, D (6.0 mm). Even at lower I_T (619.0 W/m^2), the gain in outlet air temperature (T_o) and collector efficiency (η_c) are obtained as 1.6°C and 10.5% at smaller D (6.0 mm) than larger jet hole diameter, D (8.0 mm) and D (10.0 mm) respectively for fixed $\dot{m}_1$ (0.035 kg/s). The maximum increment in heat transfer coefficient (h_{Pj}) is found as 57.9% and 82.9% at smaller D (6.0 mm) in comparison to larger jet hole diameter, D (8.0 mm) and D (10.0 mm) respectively, whereas the maximum increment in Nusselt number (Nu_{Pj}) is obtained as 52.6% and 75.0% at smaller jet hole diameter, D (6.0 mm) than larger jet hole diameter, D (8.0 mm) and D (10.0 mm) respectively for mass flow rate of air, $\dot{m}_1$ (0.064 kg/s). In order to predict the performance of the air heater, the correlations of Nusselt number are also been developed presented in this paper.

APPENDIX A

A.1 Method of Uncertainty Analysis

Heat transfer coefficient, $h_{Pj} = (\dot{m}_1 + \dot{m}_2)\ C\ (T_o - T_i) / A\ (T_P - T_{a2})$ in cross flow jet plate solar air heater is related with $\dot{m}_1$, $\dot{m}_2$, T_o, T_i, T_P and T_{a2}. However, $\dot{m}_1$ is related with the density, ρ of air and $\overline{V}_1$. Similarly, $\dot{m}_2$ is related with density, ρ of air and $\overline{V}_2$ and density, ρ with temperature, T_A. Hence, the h_{Pj} is related with T_A, $\overline{VV}_1$, $\overline{V}_2$, T_o, T_i, T_P and T_{a2}. Here, each measured quantities have some uncertainty (u) and these uncertainties creates an uncertainty in calculated result of the h_{Pj}.

By the approximation, h_{Pj} is a linear function of the independent variables, (T_A, $\overline{VV}_1$, $\overline{V}_2$, T_o, T_i, T_P and T_{a2}) and these behave like standard deviation (σ). Hence, the precision uncertainty in h_{Pj} for 95% of the confidence be,

$$P_{R_{h_{PJ}}} = \pm[\left(P_{R_{T_A}}\right)^2 + \left(P_{R_{\overline{V}_1}}\right)^2 + \left(P_{R_{\overline{V}_2}}\right)^2 + \left(P_{R_{T_o}}\right)^2 + \left(P_{R_{T_i}}\right)^2 + \left(P_{R_{T_P}}\right)^2 + \left(P_{R_{T_{a2}}}\right)^2]^{1/2} \quad (A1)$$

where, $P_{R_{h_{Pj}}} = u_{h_{Pj}}/h_{Pj}$, $P_{R_{T_A}} = u_{T_A}/T_A$, $P_{R_{\overline{V}_1}} = u_{\overline{V}_1}/\overline{V}_1$,
$P_{R_{\overline{V}_2}} = u_{\overline{V}_2}/\overline{V}_2$, $P_{R_{T_o}} = u_{T_o}/T_o$, $P_{R_{T_i}} = u_{T_i}/T_i$,
$P_{R_{T_P}} = u_{T_P}/T_P$, and $P_{R_{T_{a2}}} = u_{T_{a2}}/T_{a2}$

Likewise, the standard deviation of h_{Pj} is,

$$\sigma_{h_{Pj}}/h_{Pj} = [(\sigma_{T_A}/T_A)^2 + (\sigma_{\overline{V}_1}/\overline{V}_1)^2 + (\sigma_{\overline{V}_2}/\overline{V}_2)^2 + (\sigma_{T_o}/T_o)^2 + (\sigma_{T_i}/T_i)^2 + (\sigma_{T_P}/T_P)^2 + (\sigma_{T_{a2}}/T_{a2})^2]^{1/2} \quad \text{(A2)}$$

This approach of uncertainty has been established by S.J. Kline and F.A. McKlintock (1953). The two types of uncertainties are associated in the uncertainty of h_{Pj}. These are bias uncertainty and precision uncertainty. Both uncertainties may be considered separately. The estimate for single-sample precision uncertainty in h_{Pj} be,

$$P_{R_{h_{Pj}}}/h_{Pj} = 1.96\,(\sigma_{h_{Pj}}/h_{Pj}) \quad \text{(A3)}$$

Now after considering the bias uncertainty ($B_{h_{Pj}}/h_{Pj}$), the total uncertainty of h_{Pj} be,

$$U_{h_{Pj}} = \pm\,[(P_{R_{h_{Pj}}}/h_{Pj} + B_{h_{Pj}}/h_{Pj}]^{1/2} \quad \text{(A4)}$$

where $B_{h_{Pj}}/h_{Pj} = [(B_{T_A}/T_A)^2 + (B_{\overline{V}_1}/\overline{V}_1)^2 + (B_{\overline{V}_2}/\overline{V}_2)^2 + (B_{T_o}/T_o)^2 + (B_{T_i}/T_i)^2 + (B_{T_P}/T_P)^2 + (B_{T_{a2}}/T_{a2})^2]^{1/2}$

A.2 The Total Uncertainty in h_{Pj}

In this study, the experiments are carried out in cross flow staggered hole jet plate solar air heater for variable jet hole diameter D (6.0 mm, 8.0 mm and 10.0 mm). For D (6.0 mm, 8.0 mm and 10.0 mm), the mean values of the variables (h_{Pj}, η_c, Re_{ja2}, T_A, T_P, T_i, T_o, $\overline{VV}_1$, $\overline{V}_2$, V_j, $\overline{V}_o$, and I_T) are obtained separately for each day and the mean (of mean values of the variables) are mixed and considered together. The total uncertainty (precision and bias) of the h_{Pj} has been calculated from the Eq. (A4). The precision uncertainty of each measured quantities is found by the Eq. (A3) and the bias uncertainties of each measured quantities are taken from the manual of the measuring instruments.

NOMENCLATURE

A	surface area of absorber plate, m^2
Aj	area of jet hole, m^2
A_2	cross-sectional area of upper channel, m^2
B	bias uncertainty
C_p	specific heat capacity of air, kJ/kgK
D	diameter of jet hole, m
D_2	hydraulic diameter of upper channel, m $D_2 = 4WZ_2/2(W + Z_2)$
d	air thickness between the absorber and cover plate, m
h_{Pj}	average plate-to-jet air heat transfer coefficient, W/m^{2}K
I_T	incident solar intensity, W/m^2
k_a	thermal conductivity of air flowing through duct, W/mK
l_i	glass wool thickness, m
L	length of air heater, m
$\dot{m}_1$	mass flow rate of air in parallel plate and bottom channel, kg/s
$\dot{m}_2$	mass flow rate of air in cross flow, kg/s
N	total number of jet holes in jet plate
Nu_{Pj}	Nusselt number between absorber and jet plate
P_R	precision uncertainty
Re_{ja2}	flow Reynolds number between absorber plate and jet plate
T_A	ambient air temperature, ^{o}C
T_1	inlet temperature of air at bottom channel, ^{o}C
T_2	inlet temperature of air at upper channel, ^{o}C
T_a	channel air temperature in parallel plate air heater, ^{o}C
T_{a1}	air temperature at lower channel, ^{o}C
T_{a2}	air temperature at upper channel, ^{o}C
T_i	inlet air temperature above jet plate in mixing of air, ^{o}C
T_o	outlet air temperature, ^{o}C
T_{ol}	outlet air temperature at jet hole, ^{o}C
T_P	absorber plate temperature, ^{o}C
$\overline{VV}_1$	wetted mean inlet velocity of air in bottom channel, m/s
$\overline{V}_2$	wetted mean inlet velocity of air in the upper channel, m/s
Vj	jet air velocity, m/s
$\overline{V}$	average flow velocity of air in the upper channel, m/s
$\overline{VVV}_o$	wetted mean outlet velocity of air in the upper channel, m/s
V_w	wind velocity, m/s
$\overline{VV}_{av}$	average velocity of jet air and inlet velocity in upper channel, m/s
W	air heater width, m
X	streamwise pitch of the holes, m
Y	spanwise pitch of the holes, m
Z	total depth of solar air heater (Z_1+Z_2), m
Z_1	spacing between jet and bottom plate, m
Z_2	spacing between jet and absorber plate, m

Greek Symbols

η_c	collector efficiency
θ	angle of tilt
ρ	density of air, kg/m^3
τ	transmissivity of glass cover

Subscripts

i	inlet air at upper channel
j	jet air or, jet plate
o	outlet air at heater exit
ol	outlet air at jet hole
P	absorber plate

REFERENCES

Aboghrara, A.M., Baharudin, B.T.H.T., Alghoul, M.A., Adam, N.M., Hairuddin, A.A., and Hasan, H.A., 2017, "Performance analysis of solar air heater with jet impingement on corrugated absorber plate," *Case Studies in Thermal Engineering*, **10**, 111-120. https://dx.doi.org/10.1016/j.csite.2017.04.002

Aboghrara, A.M., Alghoul, M.A., Baharudin, B.T.H.T., Elbreki, A.M., Ammar, A.A., Sopian, K., and Hairuddin, A.A., 2018, "Parametric study on the thermal performance and optimal design elements of solar air heater enhanced with jet impingement on a corrugated absorber plate," *International Journal of Photoenergy*, **2018**, 1-22. https://dx.doi.org/10.1155/2018/1469385

Aharwal, K.R., Gandhi, B.K., and Saini, J.S., 2009, "Heat transfer and friction characteristics of solar air heater ducts having integral inclined discrete ribs on absorber plate," *International Journal of Heat and Mass Transfer*, **52**, 5970-5977. https://dx.doi.org/10.1016/j.ijheatmasstransfer.2009.05.032

Akpinar, E.K., and Kocyigit, F., 2010, "Experimental investigation of thermal performance of solar air heater having different obstacles on absorber plates," *International Communications in Heat and Mass Transfer*, **37**(4), 416-421. https://dx.doi.org/10.1016/j.icheatmasstransfer.2009.11.007

Belusko, M., Saman, W., and Bruno, F., 2008, "Performance of jet impingement in unglazed air collector," *Solar Energy,* **82**(5), 389-398. https://dx.doi.org/10.1016/j.solener.2007.10.005

Chabane, F., Moummi, N., Benramache, S., Bensahal, D., and Belahssen, O., 2013a, "Collector efficiency by single pass of solar air heaters with and without using fins," *Engineering Journal*, **17**(3), 43-55. https://dx.doi.org/10.4186/ej.2013.17.3.43

Chabane, F., Moummi, N., Brima, A., and Benramache, S., 2013b, "Thermal efficiency analysis of a single-flow solar air heater with different mass flow rates in a smooth plate," *Frontiers in Heat and Mass Transfer*, **4**, 013006, 1-6.
https://dx.doi.org/10.5098/hmt.v4.1.3006

Chabane, F., Moummi, N., and Benramache, S., 2014, "Experimental study of heat transfer and thermal performance with longitudinal fins of solar air heater," *Journal of Advanced Research*, **5**(2), 183-192.
https://dx.doi.org/10.1016/j.jare.2013.03.001

Chaudhury, C., and Garg, H.P., 1991, "Evaluation of a jet plate solar air heater," *Solar Energy*, **46**(4), 199-209.
https://dx.doi.org/10.1016/0038-092X(91)90064-4

Chauhan, R., and Thakur, N.S., 2013, "Heat transfer and friction factor correlation for impinging jet solar air heater," *Experimental Thermal and Fluid Science,* **44**, 760-767.
https://dx.doi.org/10.1016/j.expthermflusci.2012.09.019

Das, S., Biswas, A., and Das, B., 2022, "Numerical analysis of a solar air heater with jet impingement—comparison of performance between jet designs," *Journal of Solar Energy*, **144**(1), 011001.
https://dx.doi.org/10.1115/1.4051478

Farahani, S.D., and Shadi, M., 2021, "Optimization-decision making of roughened solar air heaters with impingement jets based on 3E analysis," *International Communications in Heat and Mass Transfer*, **129**, 105742.
https://dx.doi.org/10.1016/j.icheatmasstransfer.2021.105742

Flilihi, E., Sebbar, E.H., Achemlal, D., Rhafiki, T.E., Sriti, M., and Chaabelasri, E., 2022, "Effect of absorber design on convective heat transfer in a flat plate solar collector: A CFD modeling," *Frontiers in Heat and Mass Transfer*, **18**, 39, 1-6.
https://dx.doi.org/10.5098/hmt.18.39

Florschuetz, L.W., Metzger, D.E., and Truman, C.R., 1981, "Jet array impingement with cross flow-correlation of streamwise resolved flow and heat transfer distributions," *NASA Contractor Report*, **3373**.
https://ntrs.nasa.gov/api/citations/19810006721/downloads/19810006721.pdf
(Last accessed on 20th April, 2022).

Garg, H.P., Datta, G., and Bandyopadhyay, B., 1983, "A study on the effect of enhanced heat transfer area in solar air heaters," *Energy Conversion and Management*, **23**(1), 43-49.
https://dx.doi.org/10.1016/0196-8904(83)90007-9

Garg, H.P., Datta, G., and Bhargava, A.K., 1989, "Performance studies on a finned-air heater," *Energy*, **14**(2), 87-92.
https://dx.doi.org/10.1016/0360-5442(89)90082-0

Garg, H.P., Jha, R., Choudhury, C., and Datta, G., 1990, "Theoretical analysis on a new finned type solar air heater," In: Horigome, T., Kimura, K., Takakura, T., Nishino, T., and Fujii, I. (Editors), *International Solar Energy Society Proceedings Series*, Clean and Safe Energy Forever, Pergamon, 537-541.
https://dx.doi.org/10.1016/B978-0-08-037193-1.50110-5

Garg, H.P., Jha, R., Choudhury, C., and Datta, G., 1991, "Theoretical analysis on a new finned type solar air heater," *Energy*, **16**(10), 1231-1238.
https://dx.doi.org/10.1016/0360-5442(91)90152-C

Gupta, C.L., and Garg, H.P., 1967, "Performance studies on solar air heaters," *Solar Energy*, **11**(1), 25-31.
https://dx.doi.org/10.1016/0038-092X(67)90014-X

Gupta, D., Solanki, S.C., and Saini, J.S., 1993, "Heat and fluid flow in rectangular solar air heater ducts having transverse rib roughness on absorber plates," *Solar Energy*, **51**(1), 31-37.
https://dx.doi.org/10.1016/0038-092X(93)90039-Q

Hasan, H.A., Sopian, K., Jaaz, A.H., and Al-Shamani, A.N., 2017, "Experimental investigation of jet array nanofluids impingement in photovoltaic/thermal collector," *Solar Energy*, **144**, 321-334.
https://dx.doi.org/10.1016/j.solener.2017.01.036

Hassan, H., and AboElfadl, S., 2021, "Heat transfer and performance analysis of SAH having new transverse finned absorber of lateral gaps and central holes," *Solar Energy*, **227**, 236-258.
https://dx.doi.org/10.1016/j.solener.2021.08.061

Irfan, K., and Emre, T., 2006, "Experimental Investigation of solar air heater with free and fixed fins: Efficiency and exergy loss," *International Journal of Science and Technology*, **1**(1), 75-82.

Jaurker, A.R., Saini, J.S., and Gandhi, B.K., 2006, "Heat transfer and friction characteristics of solar air heater duct using rib-grooved artificial roughness," *Solar Energy*, **80**(8), 895-907.
https://dx.doi.org/10.1016/j.solener.2005.08.006

Karsli, S., 2007, "Performance analysis of new design solar air collectors for drying applications," *Renewable Energy*, **32**(10), 2007, 1645-1660.
https://dx.doi.org/10.1016/j.renene.2006.08.005

Kercher, D.M., and Tabakoff, W., 1970, "Heat transfer by a square array of round air jets impinging perpendicular to a flat surface including the effect of spent air," *Journal of Engineering for Gas Turbines and Power,* **92**(1), 73-82.
https://dx.doi.org/10.1115/1.3445306

Kline, S.J., and McKlintock, F.A., 1953, "Describing uncertainties in single sample experiments," *Mechanical Engineering*, **75**, 3-8.

Kumar, N., Kumar, A., and Maithani, R., 2020, "Development of new correlations for heat transfer and pressure loss due to internal conical ring obstacles in an impinging jet solar air heater passage," *Thermal Science and Engineering Progress*, **17**, 100493.
https://dx.doi.org/10.1016/j.tsep.2020.100493

Kumar, R., Nadda, R., Kumar, S., Kumar, K., Afzal, A., Razak, R.K.A., and Sharifpur, M., 2021a, "Heat transfer and friction factor correlations for an impinging air jets solar thermal collector with arc ribs on an absorber plate," *Sustainable Energy Technologies and Assessments*, **47**, 101523.
https://dx.doi.org/10.1016/j.seta.2021.101523

Kumar, S., Thakur, R., Suri, A.R.S., Kashyap, K., Singhy, A., Kumar, S., and Kumar, A., 2021b, "A comprehensive review of performance analysis of with and without fins solar thermal collector," *Frontiers in Heat and Mass Transfer*, **16**(4), 1-11.
https://dx.doi.org/10.5098/hmt.16.4

Kurtbas, I., and Turgut, E., 2006, "Experimental investigation of solar air heater with free and fixed fins: Efficiency and energy loss," *International Journal of Science and Technology*, **1**(1), 75-82.

Maithani, R., Sharma, S., and Kumar, A., 2021, "Thermo-hydraulic and exergy analysis of inclined impinging jets on absorber plate of solar air heater," *Renewable Energy*, **179**, 84-95.
https://dx.doi.org/10.1016/j.renene.2021.07.013

Matheswaran, M.M., Arjunan, T.V., and Somasundaram, D., 2018, "Analytical investigation of solar air heater with jet impingement usingenergy and exergy analysis," *Solar Energy*, **161**, 25-37.
https://dx.doi.org/10.1016/j.solener.2017.12.036

McAdams, W.H., 1954, *Heat Transmission*, Third edition, McGraw-Hill, New York.

Metzger, D.E., Florschuetz, L.W., Takeuchi, D.I., Behee, R.D., and Berry, R.A., 1979, "Heat transfer characteristics for inline and staggered arrays of circular jets with cross-flow of spent air," *Journal of Heat Transfer*, **101**(3), 526-531.
https://dx.doi.org/10.1115/1.3451022

Moffat, R.J., 1988, "Describing the uncertainties in experimental results," *Experimental Thermal and Fluid Science*, **1**(1), 3-17.
https://dx.doi.org/10.1016/0894-1777(88)90043-X

Moshery, R., Chai, T.Y., Sopian, K., Fudholi, A., and Al-Waeli, A.H.A., 2021, "Thermal performance of jet-impingement solar air heater with transverse ribs absorber plate," *Solar Energy*, **214**, 355-366.
https://dx.doi.org/10.1016/j.solener.2020.11.059

Nadda, R., Kumar, A., and Maithani, R., 2017, "Developing heat transfer and friction loss in an impingement jets solar air heater with multiple arc protrusion obstacles," *Solar Energy*, **158**, 117-131.
https://dx.doi.org/10.1016/j.solener.2017.09.042

Nayak, R.K., and Singh, S.N, 2016, "Effect of geometrical aspects on the performance of jet plate solar air heater," *Solar Energy*, **137**, 434-440.
https://dx.doi.org/10.1016/j.solener.2016.08.024

Nayak, R.K., Prasad, R.S., Nayak, U.K., and Gupta, A.K., 2022a, "Analytical study of thermal performance of a jet plate solar air heater with the longitudinal fins under the cross flow and non-cross flow conditions," *Frontiers in Heat and Mass Transfer*, **19**, 7, 1-12.
https://dx.doi.org/10.5098/hmt.19.7

Nayak, R.K., Prasad, R.S., Nayak, U.K., and Gupta, A.K., 2022b, "Performance analysis of longitudinal fin jet plate solar air heater under cross flow condition," *Frontiers in Heat and Mass Transfer*, **19**, 22, 1-12.
https://dx.doi.org/10.5098/hmt.19.22

Pazarlioğlu, H.K., Ekiciler, R., and Arslan, K, 2021, "Numerical analysis of effect of impinging jet on cooling of solar air heater with longitudinal fins," *Heat Transfer Research*, **52**(11), 47-61.
https://dx.doi.org/10.1615/HeatTransRes.2021037251

Perry, K.P., 1954, "Heat transfer by convection from a hot gas jet to a plane surface," *Proc. Inst. Mech. Engg.,* **168**(30), 775-780.

Prasad, B.N., and Saini, J.S., 1988, "Effect of artificial roughness on heat transfer and friction factor in a solar air heater," *Solar Energy*, **41**(6), 555-560.
https://dx.doi.org/10.1016/0038-092X(88)90058-8

Rajaseenivasan, T., Prasanth, S.R., Antony, M.S., and Srithar, K., 2017, "Experimental investigation on the performance of an impinging jet solar air heater," *Alexandria Engineering Journal*, **56**(1), 63-69.
https://dx.doi.org/10.1016/j.aej.2016.09.004

Romdhane, B.S., 2007, "The air solar collectors: Comparative study, introduction of baffles to favor the heat transfer," *Solar Energy*, **81**(1), 2007, 139-149.
https://dx.doi.org/10.1016/j.solener.2006.05.002

Sahu, M.M., and Bhagoria, J.L., 2005, "Augmentation of heat transfer coefficient by using 90º broken transverse ribs on absorber plate of solar air heater," *Renewable Energy*, **30**(13), 2057-2073.
https://dx.doi.org/10.1016/j.renene.2004.10.016

Salman, M., Chauhan, R., and Kim, S.C., 2021a, "Exergy analysis of solar heat collector with air jet impingement on dimple-shape-roughened absorber surface," *Renewable Energy*, **179**, 918-928.
https://dx.doi.org/10.1016/j.renene.2021.07.116

Salman, M., Park, M.H., Chauhan, R., and Kim, S.C., 2021b, "Experimental analysis of single loop solar heat collector with jet impingement over indented dimples," *Renewable Energy*, **169**, 618-628.
https://dx.doi.org/10.1016/j.renene.2021.01.043

Salman, M., Chauhan, R., Poongavanam, G.K., Park, M.H., and Kim, S.C., 2022, "Utilizing jet impingement on protrusion/dimple heated plate to improve the performance of double pass solar heat collector," *Renewable Energy*, **181**, 653-665.
https://dx.doi.org/10.1016/j.renene.2021.09.082

Shetty, S.P., Madhwesh, N., and Karanth, K.V., 2021, "Numerical analysis of a solar air heater with circular perforated absorber plate," *Solar Energy*, **215**, 416-433.
https://dx.doi.org/10.1016/j.solener.2020.12.053

Singh, S., Chaurasiya, S.K., Negi, B.S., Chander, S., Nemś, M., and Negi, S., 2020, "Utilizing circular jet impingement to enhance thermal performance of solar air heater," *Renewable Energy*, **154**, 1327-1345.
https://dx.doi.org/10.1016/j.renene.2020.03.095

Singh, S.N., 2006, "Performance studies on continuous longitudinal fins solar air heater," *Journal of ISM, Dhanbad*, **2**.

Sivakumar, S., Siva, K., and Mohanraj, M., 2019, "Experimental thermodynamic analysis of a forced convection solar air heater using absorber plate with pin-fins," *Journal of Thermal Analysis and Calorimetry*, **136**, 39–47.
https://dx.doi.org/10.1007/s10973-018-07998-5

Soni, A., and Singh, S.N., 2017, "Experimental analysis of geometrical parameters on the performance of an inline jet plate solar air heater," *Solar Energy*, **148**, 149-156.
https://dx.doi.org/10.1016/j.solener.2017.03.081

Sukhatme, S.P., 1996, *Solar energy, Principles of Thermal Collection and Storage*, 2nd edition, Tata McGraw Hill Publishing Company Limited, New Delhi.

Thombre, S.B., and Sukhatme, S.P., 1995, "Turbulent flow heat transfer and friction factor characteristics of shrouded fin arrays with uninterrupted fins," *Experimental Thermal and fluid Science*, **10**(3), 388-396.
https://dx.doi.org/10.1016/0894-1777(94)00059-H

Verma, R., Chandra, R., and Garg, H.P., 1991, "Parametric studies on the corrugated solar air heaters with and without cover," *Renewable Energy*, **1**(3-4), 361-371.
https://dx.doi.org/10.1016/0960-1481(91)90045-Q

Vinod, P.D., and Singh, S.N., 2017, "Thermo-hydraulic performance analysis of jet plate solar air heater under cross flow condition," *International Journal of Heat and Technology*, **35**(3), 603-610.
https://dx.doi.org/10.18280/ijht.350317

Xing, Y., Spring, S., and Weigand, B., 2010, "Experimental and numerical investigation of heat transfer characteristics of inline and staggered arrays of impinging jets," *Journal of Heat Transfer*, **132**(9), 092201.
https://dx.doi.org/10.1115/1.4001633

Yadav, S., and Saini, R.P., 2020, "Numerical investigation on the performance of a solar air heater using jet impingement with absorber plate,"*Solar Energy*, **208**, 236-248.
https://dx.doi.org/10.1016/j.solener.2020.07.088

Yadav, S., and Saini, R.P., 2022, "Thermo-hydraulic CFD analysis of impinging jet solar air heater with different jet geometries," In: Kumar, R., Pandey, A.K., Sharma, R.K., and Norkey, G. (Editors), *Recent Trends in Thermal Engineering*, Lecture Notes in Mechanical Engineering, Springer, Singapore, 193-201.
https://dx.doi.org/10.1007/978-981-16-3132-0_19